

# The Effect of Reversals for a Stochastic Source-Seeking Process Inspired by Bacterial Chemotaxis

Noele Norris\*, Filippo Menolascina<sup>†</sup>, Emilio Frazzoli\*, and Roman Stocker<sup>†</sup>

**Abstract**—Many species of bacteria are motile, but they use different random strategies to determine where to swim in response to chemical gradients. We extend past work describing a chemotactic *E. coli* cell as an ergodic, stochastic hybrid system to model a variety of different strategies. We quantify differences in asymptotic performance and show that the processes described by our models converge to stationary distributions that are proportional to various powers of the distribution of chemicals in the environment. Our main goal is to understand the implications of the differences between *E. coli*'s chemotaxis strategy and the more complicated strategy of the marine bacterium *Vibrio alginolyticus*, which, unlike *E. coli*, can swim both forward and backward. We argue that *Vibrio*'s ability to reverse allows it to accumulate more tightly around nutrient sources, and we quantify the effects that reversals have on the stationary distribution of various processes. Our results provide intuition for designing minimalistic multi-agent robotic systems that are better suited for source-seeking tasks in particular environments.

## I. INTRODUCTION

Bacterial chemotaxis is the process in which motile bacteria, such as *E. coli*, bias their swimming in response to gradients of chemical concentrations. An *E. coli* cell's ability to follow gradients is severely limited by its tiny size. Only about two microns long, the cell is jostled about by the Brownian motion of the water molecules and, therefore, cannot swim straight. "After about 10 seconds, it drifts off course by more than 90 degrees, and thus forgets where it is going" [1]. Yet, populations of *E. coli* cells use temporal measurements of the environment to successfully distribute themselves in accordance to distributions of nutrient concentrations.

Many engineers have been inspired by *E. coli*'s simple yet elegant chemotactic strategy. (For examples, see [2], [3], and references therein.) In [4], Mesquita modeled a chemotactic cell as a *stochastic hybrid system*, as formulated in [5], and showed that, without using any communication or knowledge of position, a population of identical, independently-acting chemotactic agents converges to the *ideal free distribution*. This is the distribution that is proportional to the distribution of the chemicals. Thus, it is 'ideal' because, in the case in which the chemicals are nutrients, it is the distribution in which each agent has an equal share of the nutrients [6].

The key to the success of *E. coli*'s chemotactic strategy is its stochastic nature. In this strategy, a cell 'runs' forward with exponentially distributed run times and then 'tumbles'

\*The authors are with the Laboratory for Information and Decision Systems, MIT, Cambridge, MA, USA. (norrisn@mit.edu, frazzoli@mit.edu)

<sup>†</sup>The authors are with the Ralph M. Parsons Laboratory, Department of Civil and Environmental Engineering, MIT, Cambridge, MA, USA. (romans@mit.edu, filipm@mit.edu)

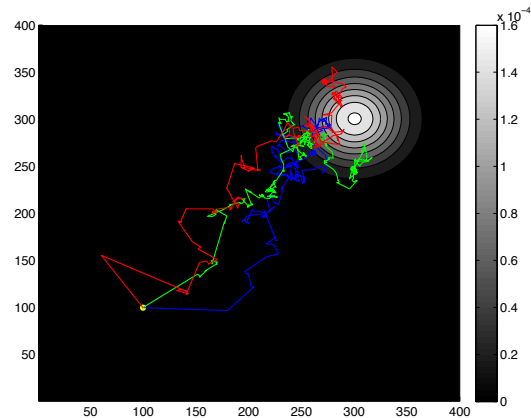


Fig. 1. Trajectories of three simulated cells following the gradient of a Gaussian-distributed nutrient patch. The three cells have identical parameters, imitating a run-and-tumble strategy. The yellow dot marks their shared initial position, while the other dots mark their final positions.

to reorient itself. It chooses a new orientation with almost uniform probability before starting a new run. If the environment is isotropic, the cell's behavior is that of a simple random walk. But, when the cell senses an uphill gradient of nutrient concentrations, it modifies its run time by decreasing the probability of tumbling. This makes it more likely that the cell will continue to swim towards higher concentrations of nutrients. However, as this strategy is probabilistic, a cell will still often swim down gradient, as seen in Figure 1.

The stochasticity of this 'run-and-tumble' control strategy has very important implications. In [4], Mesquita used the theory developed by Davis in [7] and Jacobsen in [8] to show that this process is a so-called "piecewise deterministic Markov process." Because the system can be described as a continuous Markov process, Mesquita used stochastic stability theory, as developed by Meyn and Tweedie in [9] and [10], to prove that the process is ergodic and, thus, converges to a unique stationary distribution. Therefore, by the pathwise ergodic theorem [11], we can sample the position of the process at uniform time intervals to estimate the stationary distribution of the process. And because this process converges to the ideal free distribution, we can use the position measurements over time of a population of agents to learn the distribution of chemicals in an environment. This stochastic strategy is advantageous because its ergodicity does not allow the system to become trapped at local maxima. Instead, the distribution of the agents will ultimately reflect the relative magnitudes of all chemical sources. Also, because of its

simplicity, this source-seeking strategy can be achieved using a multi-agent system comprised of very cheap, minimalistic robots.

In this paper, we extend Mesquita’s results in light of new experimental results on the marine bacterium *Vibrio alginolyticus*. *Vibrio* uses a chemotaxis strategy quite different from that of *E. coli*. Experimentalists have observed that a population of *Vibrio* cells, although swimming much faster than *E. coli* cells, accumulates much more tightly around nutrient patches [12]. We argue that this tighter accumulation occurs because, unlike *E. coli*, *Vibrio* can swim in reverse. While the *E. coli* motility strategy is comprised of two steps—a run and a reorientation, the *Vibrio* strategy adds a third step: a reversal in between its run and reorientation steps. In what has been called its “reverse-and-flick” swimming pattern, a *Vibrio* cell swims in some direction for some random amount of time, then reverses and backtracks for another random time interval, and then ‘flicks’ by 90 degrees on average before again swimming forward [13].

*Vibrio*’s environment, the ocean, is a much harsher environment than *E. coli*’s regular environment within the gut. In the ocean, nutrients are sparse, and the turbulence of the waves cause them to dissipate quickly [14], [15]. How does *Vibrio*’s chemotactic strategy reflect these environmental differences? Can *Vibrio*’s strategy teach us anything about optimizing, or at least improving, stochastic source-seeking strategies for specific environments? Our goal is to characterize differences in the performance of various bacterial motility strategies to gain intuition about why particular species, living in particular environments, have evolved certain chemotactic strategies. Once gained, these insights can be used to engineer minimalistic, source-seeking systems that are better suited for specific environments.

In this paper, we present results from [16]. We generalize Mesquita’s model of two-step, run-and-tumble processes to assess the effect of biases in reorientation. In our generalization, the sequence of orientation states is no longer memoryless. We show that all two-step strategies described by our model converge to distributions proportional to  $q^n(x)$ , for some  $n > 0$ , where  $q(x)$  is the amount of nutrients at location  $x$ . We show that, without changing the sensitivity of the sensing process, we can modify the value of  $n$  by a factor in the interval  $(0, 2)$  by biasing the reorientation angles chosen during each tumble to favor either reversing or continuing forward. This analysis shows that favoring reversing increases the value of  $n$  by at most a factor of two. This provides insight for the expected performance of more complicated three-step, run-reverse-flick processes. Although we do not have an analytical solution for the stationary distribution of a general three-step process, we do solve for the stationary distribution of a simplified three-step process in a particular environment. In this scenario, the three-step process does achieve the accumulation factor of two. We also provide a few simulation results of general three-step processes, which suggest that a run-reverse-flick strategy may be more robust to noise and system inaccuracies.

## II. MODEL

To model various chemotactic strategies, we extend the hybrid system model given in [4].

*State space:* Restricting our analysis to the two-dimensional Cartesian plane, we consider a process with position  $x \in X$ , a compact set of  $\mathbb{R}^2$ , and orientation  $v \in \mathbb{S}$ , the unit circle:  $\mathbb{S} = \{v \in \mathbb{R}^2 : \|v\|_2 = 1\}$ . We take  $l$  to be the normalized two-dimensional Lebesgue measure on  $\mathbb{X}$  and  $\nu$  to be the normalized one-dimensional Lebesgue measure on  $\mathbb{S}$ . Thus,  $l(X) = 1$ ,  $\text{supp } l = X$ ,  $\nu(\mathbb{S}) = 1$ , and  $\text{supp } \nu = \mathbb{S}$ , so, if  $p(x, v, t)$  is the probability that the process is at location  $x$  with velocity  $v$  at time  $t$ ,  $\int_{X \times \mathbb{S}} p(x, v, t) l(dx) \nu(dv) = 1$ .

The two-step process has state  $(x, v) \in X \times \mathbb{M}_2$ , where  $\mathbb{M}_2 := \mathbb{S}$ . The three-step process has state  $(x, d, v) \in X \times \mathbb{M}_3$ , where  $\mathbb{M}_3 := \{-1, +1\} \times \mathbb{S}$ . The direction  $d$  is needed to keep track of whether the process is moving forward,  $d = +1$ , or reversing,  $d = -1$ . We consider a general two- or three-step process to have state  $(x, m) \in X \times \mathbb{M}$ , where  $\mathbb{M}$  is equal to either  $\mathbb{M}_2$  or  $\mathbb{M}_3$ .

*Flow:* The process has continuous dynamics and is piecewise-linear. Thus, when the two-step or three-step process has orientation  $v$ , it flows according to

$$\frac{dx}{dt} = f(x, v) = f(v) = v. \quad (1)$$

We thus assume unit speed. Notice that, for all  $x$ ,  $\int_{\mathbb{S}} f(x, v) \nu(dv) = 0$ . Thus, unconditioned on measurements or initial position, a process is equally likely to have any orientation  $v$  and can explore its environment by moving in any direction with equal probability. This allows us to prove that the process is ergodic.

*Jump rate:* To allow direct comparison, we assume that *Vibrio*-like strategies share the same jump rate characteristics with *E. coli*. Thus, we assume that both two-step and three-step processes have exponentially distributed run times with parameter  $\lambda(x, m)$ . Thus, the conditional probability that no jump occurs between time  $t_1$  and  $t_2$  given that the process is at position  $x(t_1)$  and orientation  $v(t_1)$  at time  $t_1$  is

$$\exp\left(-\int_{t_1}^{t_2} \lambda(\varphi_{t_2-t_1}(x(t_1), v(t_1)), v(t_1)) d\tau\right),$$

where  $\varphi_t(x, v) = x + vt \in \mathbb{R}^2$  is the location of the cell after time  $t$  when moving with velocity  $v$  from initial position  $x$ .

We assume that the jump rate parameter depends on the state of the process according to the equation

$$\lambda(x, m) = a\left(M(t) - f(x, m) \cdot \nabla_x \ln q(x)\right), \quad (2)$$

where  $a > 0$  and  $M(t)$  ensures that the jump rate is positive. We can either take  $M(t) = M$  sufficiently large or, for a more efficient policy, update  $M(t)$  online, as described in [4]. Notice that it is only in the jump rate that measurements of the environment are used; the system performs chemotaxis only by modifying the probability distribution of run times. Because we assume that the system measures the gradient of the logarithm of the nutrient distribution, it exhibits *fold*

*change detection* [17], [18]. That is, it responds only to relative changes and thus modifies its response not according to the absolute amplitude of the nutrient source but according to the spatial distribution of the source.

*Transition probability:* When the process jumps, the new orientation state  $m$  depends only on the current orientation state  $m'$ . There are no instantaneous jumps in position,  $x$ .

For two-step processes, as we are interested in understanding the effects of forward persistence and reversals in motility strategies, we analyze probability density functions of the following form:

$$T(v, v') = b_F \delta(v - v') + b_R \delta(v + v') + 1 - b_F - b_R, \quad (3)$$

where  $\delta(\cdot)$  is the Dirac delta function,  $b_F$  is the forward bias,  $b_R$  is the backward bias,  $b_F, b_R \in [0, 1]$  and  $b_F + b_R \leq 1$ .

For three-step processes, we will analyze probability density functions of a few different forms. However, as a simple, base case, we assume that with probability of flicking  $p_F$  the process chooses with uniform probability a new orientation and with probability  $1 - p_F$  keeps it same orientation:

$$T[(d, v), (d', v')] = \begin{cases} 0 & \text{if } d = d'; \\ \delta(v + v') & \text{if } d = -1, d' = +1; \\ p_F + (1 - p_F)\delta(v + v') & \text{if } d = +1, d' = -1. \end{cases} \quad (4)$$

This form is inspired by experimental results in [19] that showed that a *Vibrio* cell's swimming speed affects the probability that it will reorient after a reversal.

### III. CONVERGENCE OF TWO- AND THREE-STEP PROCESSES

In [4], Mesquita proved the ergodicity of two-step processes. By showing that the Markov process is Harris recurrent, it immediately follows that the process converges to a unique stationary distribution [20]. We can use the same approach to show ergodicity of a three-step process.

*Proposition 1:* Each two- and three-step process that can be described by our model is ergodic and thus converges to a unique stationary distribution.

*Proof:* The ergodicity of two-step processes is shown in [4]. We can use this same analysis to show the ergodicity of a three-step process. Although the transition probability of a three-step process requires that the process alternate its direction,  $d$ , at each jump, the process is irreducible because the jump rate ensures that there is a positive probability that a jump will occur within any positive time interval and the process can jump to any velocity  $v \in \mathbb{S}$  within two jumps. Harris recurrence thus follows, as shown in [16]. ■

Given that a process has a unique stationary distribution, we can determine what that stationary distribution is by finding the form of the differential equation that describes the evolution of the process and solving that equation with  $p_s(x, m, t) = p_s(x, m)$ , so that  $\partial p_s(x, m, t)/\partial t = 0$ . Mesquita used the analysis presented in [21] to show that the transport equation given in [22] is indeed the *master equation* ([23]) describing the evolution of the probability

density function of the process,  $p(x, m, t)$ . Using this same analysis, we can immediately determine that the same equation describes both our two- and three-step processes.

*Proposition 2:* A function  $p(x, m, t)$  is a probability density function of a two- or three-step process as described by our model if it satisfies the following Fokker-Planck-Kolmogorov (FPK) evolution equation:

$$\begin{aligned} \frac{\partial p(x, m, t)}{\partial t} &= -\nabla_x \cdot [f(x, m)p(x, m, t)] \\ &- \lambda(x, m)p(x, m, t) \\ &+ \int_{\mathbb{M}} T(m, m')\lambda(x, m')p(x, m', t)\nu(dm'). \end{aligned} \quad (5)$$

The first term of this FPK equation is a drift term describing the continuous motion of the process in the position state space,  $X$ ; the second term is a jump term describing the density of jumps leaving the state  $(x, m)$  at time  $t$ ; and the final term is another jump term describing the density of jumps from any other state  $(x, m')$  to the state  $(x, m)$ .

### IV. STATIONARY DISTRIBUTION OF TWO-STEP PROCESSES

As shown in [4], we can use Equation (5) directly to solve for the stationary distribution of two-step processes.

*Theorem 1:* The stationary distribution of a two-step process described by our model in an environment with nutrient distribution  $q(x)$  is

$$p_s(x, v) = p_s(x) \propto q(x)^{a(1+b_R-b_F)} \quad (6)$$

*Proof:* By Proposition 1, the stationary distribution is unique, so we can guess a solution. Plugging the parameter values into Equation 5 with  $p(x, v, t) = p_s(x)$ , we use the facts that  $\int_{\mathbb{S}} f(v')\nu(dv') = 0$  and  $f(v) = -f(-v)$  to obtain the requirement

$$0 = f(v) \cdot [-\nabla_x p_s(x) + a p_s(x)(1 + b_R - b_F)\nabla_x \ln q(x)].$$

This holds when  $\nabla_x \ln p_s(x) = a(1 + b_R - b_F)\nabla_x \ln q(x)$ . ■

Alternatively, we can use Equation 5 to see that many different strategies result in the same stationary distribution. Taking  $\lambda(x, v)$  as above, we now solve for functions  $T(\cdot, \cdot)$  that give a stationary distribution of  $p_s(x) = q^n(x)$ , where  $n > 0$ . From the FPK equation, the requirement is that:

$$\begin{aligned} (n - a)q^{a-1}(x)\nabla_x q(x) \cdot f(v) + M &= \\ \int_{\mathbb{S}} T(v, v')[M - aq^{a-1}(x)\nabla_x q(x) \cdot f(v')]\nu(dv'). \end{aligned}$$

This is satisfied when the following two equations hold:

$$\int_{\mathbb{S}} T(v, v')\nu(dv') = 1, \quad (7)$$

$$\int_{\mathbb{S}} T(v, v')f(v')\nu(dv') = \frac{a - n}{a}f(v). \quad (8)$$

Our generalization of two-step processes has retained many of the nice features seen in [4]; their stationary distributions are independent of both the orientation state,  $v$ , and the jump rate constant,  $M$ .

Theorem 1 shows that, as the reverse bias  $b_R$  increases, the process will accumulate more tightly around a chemical source, and, as the forward bias  $b_F$  increases, the process will further spread out. If either  $b_R$  or  $b_F$  equals one, the process is trapped on a one-dimensional manifold of the space  $X$  and cannot achieve the stationary distribution. Thus, modifying the values of  $b_R$  and  $b_F$  can at most change the accumulation factor by a factor of  $b \in (0, 2)$ . With a much simpler mathematical model and derivation, we thus recover a result from [24].

The stationary distribution given in Equation 6 suggests that we can achieve any accumulation factor by scaling the parameter  $a$  in the jump rate; this is what is done in [4]. However, increasing  $a$  requires greater sensitivity in sensing, as it forces the agent to measure larger exponents of the chemical concentrations. Biasing the reorientation mechanism thus provides us with an alternative method for achieving tighter accumulations without requiring more sophisticated sensors.

## V. STATIONARY DISTRIBUTION OF THREE-STEP PROCESSES?

Because the stationary distribution of a two-step process is independent of the orientation state, we could easily use the FPK equation to determine its value. However, this is unfortunately not the case for three-step processes. A new complication emerges because, with the extra step, the stationary distribution of a three-step process must simultaneously satisfy two FPK equations.

Let us assume the form of  $T(\cdot, \cdot)$  given in the model and that the probability of flicking,  $p_F$ , is one. When the process is in reverse, in state  $(x, -1, v)$ , the FPK equation requires that, if  $p_s$  is a stationary distribution, then

$$\begin{aligned} 0 &= -f(v) \cdot \nabla_x p_s(x, -1, v) \\ &+ M[p_s(x, +1, -v) - p_s(x, -1, v)] \\ &+ f(v) \cdot \frac{\nabla_x q(x)}{q(x)} [p_s(x, -1, v) + p_s(x, +1, -v)]. \end{aligned} \quad (9)$$

On the other hand, when the process is going forward, in state  $(x, +1, v)$ , the FPK equation requires:

$$\begin{aligned} 0 &= -f(v) \cdot \nabla_x p_s(x, +1, v) \\ &+ M \left[ \int_{\mathbb{S}} p_s(x, -1, v') \nu(dv') - p_s(x, +1, v) \right] \\ &+ \frac{\nabla_x q(x)}{q(x)} \cdot \left[ p_s(x, +1, v) f(v) \right. \\ &\left. - \int_{\mathbb{S}} f(v') p_s(x, -1, v') \nu(dv') \right]. \end{aligned} \quad (10)$$

If the stationary distribution were independent of the orientation state, i.e.,  $p_s(x, m) = p_s(x)$ , then Equation 9 requires that  $p_s(x) \propto q^2(x)$ , while Equation 10 requires that  $p_s(x) \propto q(x)$ . Thus, the stationary distribution of three-step processes depends on the orientation state.

Furthermore, to cancel out the jump rate constant  $M$  in both equations, we must have that both

- 1)  $p_s(x, +1, v) = p_s(x, -1, -v)$  for all  $x \in X$  and  $v \in \mathbb{S}$ , and
- 2)  $p_s(x, +1, v) = \int_{\mathbb{S}} p_s(x, -1, v') \nu(dv')$  for all  $x \in X$  and  $v \in \mathbb{S}$ .

These two conditions only hold when  $p_s$  is independent of orientation state  $m$ . Thus, the stationary distribution of a three-step process also depends on the jump rate constant.

### A. A simplified three-step process

Because of these added complications, an analytical solution for the stationary distribution of a three-step process based on the FPK is not available at this time for general environments. However, to provide some intuition for how the stationary distribution of a three-step process depends on its orientation state and jump rate constant, here we determine the stationary distribution of a very simplified three-step process in a particular (though, unfortunately, unnatural) environment. The form of the environment allows us to guess that the stationary distribution is of form  $p_s(x, m) = \alpha(x)\beta(m)$ . To make solving for  $\beta$  easier, we use a very simplified orientation state space, in which now the process's orientation must be one of the four cardinal directions.

In this simplified three-step process:

- 1) The state is  $(x, d, \theta) \in \mathbb{R}^2 \times \{-1, +1\} \times \{0, \frac{\pi}{2}, \pi, \frac{3\pi}{2}\}$ .
- 2) The continuous dynamics is described by the flow,
$$\dot{x} = f(x, d, \theta) = f(\theta) = \begin{bmatrix} \cos \theta \\ \sin \theta \end{bmatrix}.$$
- 3) The jump intensity rate is as before:
$$\lambda(x, d, \theta) = M - f(\theta) \cdot \nabla_x \ln q(x).$$
- 4) The jump kernel is:

$$\begin{aligned} T_x[(d, \theta), (d', \theta')] &= \begin{cases} 0 & \text{if } d' = d; \\ \delta(\theta' - \theta - \pi) & \text{if } d = -1, d' = +1; \\ \delta(\theta' - \theta - \frac{\pi}{2}) & \text{if } d = +1, d' = -1. \end{cases} \end{aligned}$$

That is, in this simplified three-step process, the process must always 'flick' by exactly 90 degrees.

To ensure that the stationary distribution can be written as  $p_s(x, d, \theta) = \alpha(x)\beta(d, \theta)$ , we must have that the jump intensity rate is independent of state location  $x$ . This occurs only if  $\nabla_x \ln q(x)$  is equal to a constant. To clearly show how the direction of increased gradient effects the stationary distribution, we choose  $q(x) = q(x_1, x_2) = \exp(ax_1)$ , giving  $\nabla_x \ln q(x) = [a \ 0]$ . We require that  $M \geq |a|$  to ensure that  $\lambda(x, m)$  is positive for all  $x$  and  $m$ .

Because we can use the same techniques as in Proposition 1 to prove that this process converges to a unique stationary distribution, we guess the form of the stationary distribution and check to ensure that it satisfies Equations 9 and 10. Guessing that  $p_s(x, d, \theta) \propto q^2(x)\beta(d, \theta)$  and plugging into Equation 9, we get that  $\beta(\theta, -1) = \beta(\theta + \pi, +1)$ , implying that the process, spends, on average, equal time in forward and in reverse. Now we use Equation 10 and luckily obtain a consistent set of equations for  $\beta$ . Solving these equations,

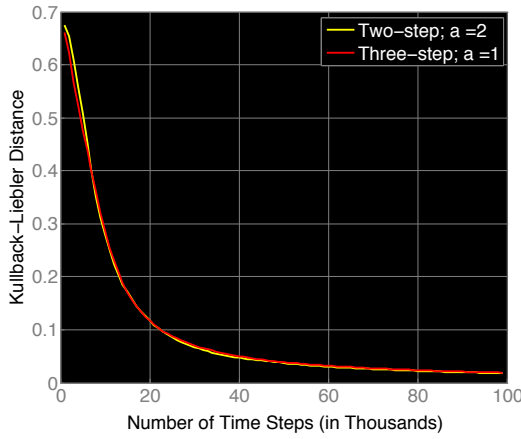


Fig. 2. **Convergence of two-step and three-step processes.** The KL distances over time between empirical averages of processes and  $q^2(x)$ . The two processes considered are a two-step process with no forward or backward bias and  $a = 2$  and a three-step process with  $a = 1$  and  $p_F = 1$ . Both processes seem to converge with the same rate.

we obtain that the stationary distribution is

$$p_s(x, d, \theta) \propto q^2(x)\beta(d, \theta), \text{ where}$$

$$\beta(0, -1) = \beta(\pi, +1) = \frac{M(M+a)}{4(2M^2 - a^2)},$$

$$\beta(\pi, -1) = \beta(0, +1) = \frac{M(M-a)}{4(2M^2 - a^2)},$$

$$\text{and } \beta\left(\frac{\pi}{2}, -1\right) = \beta\left(\frac{3\pi}{2}, -1\right) = \beta\left(\frac{\pi}{2}, +1\right) = \beta\left(\frac{3\pi}{2}, +1\right) = \frac{(M+a)(M-a)}{4(2M^2 - a^2)}.$$

The process is thus more likely to move backward than to move forward toward higher concentrations. As  $M \downarrow |a|$ , the process spends a greater percentage of its time either moving backward toward higher concentrations or forward toward lower concentrations. However, if  $M \gg |a|$ ,  $\beta(\theta, v) \approx \frac{1}{8}$ , and the process spends equal amount of time in each direction.

## VI. SIMULATIONS

In all of our simulations of three-step processes, the distributions seem to converge to a value  $h(x, m)$ , where

$$\int_{\mathbb{M}_3} h(x, m)\nu(dm) \propto q^{2a}(x).$$

To see this, we follow [4] and measure performance using a Kullback-Liebler (KL) divergence measure, which gives a distance between two probability densities. The KL distance between the actual distribution  $p_1(x)$  and a predicted distribution  $p_2(x)$  at time  $t$  is

$$H(t) = - \int_{\mathbb{R}^2} p_1(x, t) \ln \frac{p_1(x, t)}{p_1(x, t)/2 + p_2(x, t)/2} dx \geq 0.$$

If  $p_1(x, t) \rightarrow p_2(x, t)$  as  $t \rightarrow \infty$ ,  $H(t) \rightarrow 0$ . In the simulations, we take  $p_1(x, t)$  to be the empirical average of the positions of all agents over the time interval  $[0, t]$ , using summation over a grid to approximate the integration.

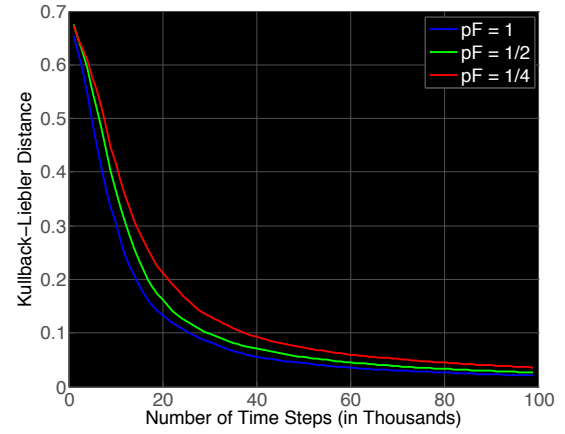


Fig. 3. **Effects of the probability of flicking on convergence rate of three-step process.** As a run-reverse system's probability of flicking decreases, its convergence rate slightly decreases.

In the simulations, we use a Cartesian environment that is 400x400 units. To avoid complications at boundaries, we identify edges so that the environment is a torus. Because the cells respond to measurements of their environment by modifying their jump rates, the time discretization used in the simulations is very important. In these simulations, we take the speed of the cells to be one position unit per time unit and the time discretization to be  $dt = 0.05$  time units per time step. So that the cells can more efficiently diffuse through the environment, we initialize the cells with a small jump rate parameter  $M(0) = 0.001$  and then update  $M(t)$  online to ensure that the jump rate remains positive. We take the simulation environment to contain a Gaussian-distributed nutrient patch described by the equation

$$q(x_1, x_2) = \frac{1}{2\pi\sigma_{x_1}\sigma_{x_2}} \exp\left(-\frac{(x_1 - c_1)^2}{2\sigma_{x_1}^2} - \frac{(x_2 - c_2)^2}{2\sigma_{x_2}^2}\right),$$

where we take  $c_1 = c_2 = 200$  and  $\sigma_{x_1} = \sigma_{x_2} = 500/16$ . In our simplified simulations, the environment is static; the nutrients do not dissipate. Furthermore, we do not simulate Brownian noise. There is no uncertainty in the dynamics or measurements of the agents.

### A. A two-step versus a three-step process

Intuitively, it may seem that reversing strategies pay too high a price to more tightly accumulate around nutrient sources. By reversing, they 'waste' time backtracking instead of simply following the source. However, the simulation shown in Figure 2 shows that the drift velocity of a run-reverse-flick process is no less than that of a run-tumble process that scales its jump rate to  $a = 2$ . The simulation furthermore suggests that both processes converge to very similar stationary distributions proportional to  $q^2(x)$ .

### B. Added robustness?

If there is an imperfection in the reorientation mechanism of a two-step process, a bias may appear in the transition probabilities causing the process to favor reversing of continuing forward. As shown in Theorem 1, this would cause

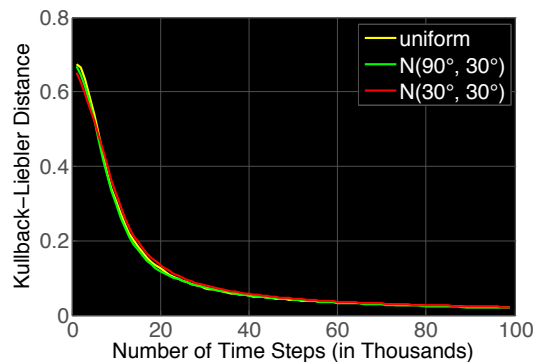


Fig. 4. **Effects of reorientation biases on convergence rate.** The simulation shows that the reorientation bias of a three-step process has little effect on the convergence rate, as long as the mechanism for reorientations allows full exploration of the space.

the process to converge to a different, possibly unknown stationary distribution. However, simulations of three-step processes suggest a robustness to uncertainties in the reorientation mechanism. This perhaps gives reversing strategies a greater advantage.

1) *Modifying probability of flicking:* Figures 3 shows that decreasing the probability of flick has very little effect on the overall performance of a run-reverse-flick system. As long as the probability of flick is greater than zero—so that the system does not become trapped on a linear manifold, the system seems to converge to the desired stationary distribution. Convergence speed decreases as the probability of flick decreases because it takes longer for the system to align itself with the measured nutrient gradient.

2) *Modifying probability density of orientations of flicks:* Figures 4 suggests that there is very little advantage to be gained from very precise reorientation mechanisms for run-reverse-flick processes. A system that favors 30 degree flicks performs almost as well as a system that favors 90 degree flicks or just uniformly tumbles after a reversal.

## VII. FUTURE WORK

In this work, we suggest that marine bacteria, such as *Vibrio*, have evolved more complicated reversing strategies because they allow for tighter accumulation and are more robust to noise and inaccuracies in reorientation. But there is much work to be done to fully understand the implications of these evolved reversing strategies. We are currently working on methods to more rigorously characterize the performance of three-step processes. We hope that numerical analysis of the FPK equation will give further insight into how the stationary distribution of three-step processes depends on the orientation state. We are also trying to derive rigorous diffusion approximations (as in [22]) that will enable us to easily characterize strategies in terms of their diffusivity and chemotactic drift rate.

Populations of motile bacteria are so impressive because they can achieve particular distributions using only local measurements of the environment. Cells require no knowledge of their position or communication capabilities. As we

better understand why a particular evolved motility strategy is optimal for a particular environment, we can gain intuition on how to engineer minimalistic multi-agent robotic systems that are as successful as bacteria.

## REFERENCES

- [1] H. C. Berg, *E. Coli in Motion*. New York: Springer Verlag, 2004.
- [2] S.-J. Liu and M. Krstic, *Stochastic Averaging and Stochastic Extremum Seeking*. Springer, June 2012.
- [3] A. R. Mesquita, J. P. Hespanha, and K. Åström, “Optimotaxis: A stochastic multi-agent optimization procedure with point measurements,” in *Hybrid Systems: Computation and Control*, M. Egerstedt and B. Mishra, Eds. Springer, 2008, pp. 358–371.
- [4] A. R. Mesquita, “Exploiting Stochasticity in Multi-agent Systems,” Ph.D. dissertation, University of California, Santa Barbara, 2010.
- [5] J. P. Hespanha, “A model for stochastic hybrid systems with application to communication networks,” *Nonlinear Analysis-Theory Methods & Applications*, vol. 62, no. 8, pp. 1353–1383, 2005.
- [6] A. Kacelnik, J. R. Krebs, and C. Bernstein, “The ideal free distribution and predator-prey populations,” *Trends in Ecology & Evolution*, vol. 7, no. 2, p. 50, 1992.
- [7] M. Davis, *Markov Models & Optimization*. Boca Raton: Chapman & Hall/CRC, 1993.
- [8] M. Jacobsen, *Point Process Theory and Applications*, ser. Marked Point and Piecewise Deterministic Processes. Boston: Birkhauser, 2006.
- [9] S. P. Meyn and R. L. Tweedie, “Stability of Markovian processes II: Continuous-time processes and sampled chains,” *Advances in Applied Probability*, pp. 487–517, 1993.
- [10] S. Meyn and R. L. Tweedie, *Markov Chains and Stochastic Stability*. Cambridge University Press, 2009.
- [11] O. Hernández-Lerma and J. B. Lasserre, *Markov Chains and Invariant Probabilities*. Springer, 2003.
- [12] L. Xie, T. Altindal, S. Chattopadhyay, and X.-L. Wu, “Bacterial flagellum as a propeller and as a rudder for efficient chemotaxis,” *Proceedings of the National Academy of Sciences*, vol. 108, no. 6, pp. 2246–2251, Jan. 2011.
- [13] R. Stocker, “Reverse and flick: Hybrid locomotion in bacteria,” *Proceedings of the National Academy of Sciences*, vol. 108, no. 7, pp. 2635–2636, Feb. 2011.
- [14] —, “Marine Microbes See a Sea of Gradients,” *Science*, vol. 338, no. 6107, pp. 628–633, Nov. 2012.
- [15] R. Stocker, J. R. Seymour, A. Samadani, D. E. Hunt, and M. F. Polz, “Rapid chemotactic response enables marine bacteria to exploit ephemeral microscale nutrient patches,” *Proceedings of the National Academy of Sciences*, vol. 105, no. 11, pp. 4209–4214, 2008.
- [16] N. Norris, “Exploring the Optimality of Various Bacterial Motility Strategies: a Stochastic Hybrid Systems Approach,” Master’s thesis, Massachusetts Institute of Technology, Cambridge, 2013.
- [17] M. D. Lazova, T. Ahmed, D. Bellomo, R. Stocker, and T. S. Shimizu, “Response rescaling in bacterial chemotaxis,” *Proceedings of the National Academy of Sciences*, vol. 108, no. 33, pp. 13 870–13 875, 2011.
- [18] O. Shoval, L. Goentoro, Y. Hart, A. Mayo, E. Sontag, and U. Alon, “Fold-change detection and scalar symmetry of sensory input fields,” *Proceedings of the National Academy of Sciences*, vol. 107, no. 36, pp. 15 995–16 000, 2010.
- [19] K. Son, J. S. Guasto, and R. Stocker, “Bacteria can exploit a flagellar buckling instability to change direction,” *Nature Physics*, July 2013.
- [20] T. E. Harris, “The existence of stationary measures for certain Markov processes,” in *Third Berkeley Symposium*, 1956, pp. 113–124.
- [21] J. Bect, “A unifying formulation of the Fokker-Planck-Kolmogorov equation for general stochastic hybrid systems,” *Nonlinear Analysis: Hybrid Systems*, vol. 4, no. 2, pp. 357–370, 2010.
- [22] H. G. Othmer and T. Hillen, “The diffusion limit of transport equations derived from velocity-jump processes,” *Siam Journal on Applied Mathematics*, vol. 61, no. 3, pp. 751–775, 2000.
- [23] N. G. Van Kampen, *Stochastic Processes in Physics and Chemistry*, 3rd ed. Amsterdam: Elsevier, 2007.
- [24] D. Grunbaum, “Advection-diffusion equations for generalized tactic searching behaviors,” *Journal of Mathematical Biology*, vol. 38, no. 2, pp. 169–194, 1999.